

Transdermal delivery of triptolide–phospholipid complex to treat rheumatoid arthritis

Xin-Yi Liu, Wen-Jun Pei, Ye-Zhen Wu, Fang-Li Ren, Si-Yu Yang and Xiu Wang 

Faculty of Pharmacy, Bengbu Medical College, Bengbu, PR China

ABSTRACT

The aim of this study was to develop and evaluate a triptolide phospholipid complex (TPCX) for the treatment of rheumatoid arthritis (RA) by transdermal delivery. TPCX was prepared and characterized by differential scanning calorimetry (DSC), Fourier-transform infrared spectroscopy (FTIR) analysis, transmission electron microscope (TEM), and scanning electron microscope (SEM). The solubility of TPCX was determined. Then, a TPCX cream was prepared to evaluate its percutaneous permeability and the antiarthritic effect. The transdermal permeability was determined using the Franz method, and a microdialysis system was used for skin pharmacokinetic study. A rat model of RA was prepared to evaluate the pharmacological effects. TPCX increased the solubility of triptolide in water, and the percutaneous permeability of TPCX cream was greatly enhanced compared with triptolide cream. The skin pharmacokinetic study indicated that TPCX cream has a longer biological half-life ($t_{1/2}$) and mean residence time (MRT), but it has a shorter T_{max} than that of triptolide cream *in vivo*. The area under the curve (AUC_{0-t})/ $AUC_{0-\infty}$) and the peak concentration (C_{max}) of TPCX cream were obviously higher than those of triptolide cream. The TPCX-loaded cream alleviated paw swelling and slowed down the progression of arthritis by inhibiting the inflammatory response by down regulating the TNF- α , IL-1 β , and IL-6 levels, thus exhibiting excellent antiarthritic effects. In summary, the prepared TPCX effectively increases the hydrophilicity of triptolide, which is good for its percutaneous absorption and enhances its effect on RA rats. TPCX can be a good candidate for the transdermal delivery to treat RA.

ARTICLE HISTORY

Received 18 July 2021
Revised 16 September 2021
Accepted 20 September 2021

KEYWORDS

Triptolide; phospholipid complex; transdermal drug delivery system (TDDS); rheumatoid arthritis; drug delivery



1. Introduction


Rheumatoid arthritis (RA) is an autoimmune inflammatory disease, and it is a leading cause of disability. The main manifestations of RA are persistent synovitis, progressive cartilage destruction, and osteoporosis. RA affects about 1% of the population, and it is associated with a large number of medical resources (Feldmann, 2002; Malahias et al., 2012; Yang et al., 2017). Triptolide, a diterpene epoxide, exhibits diverse pharmacological activities, including antirheumatic, analgesic, anti-inflammatory, immunosuppressive, and antitumor activities (Liu, 2011; Li et al., 2016). It has also been shown to be very effective against many autoimmune and inflammatory diseases, especially RA (Fan et al., 2018). Triptolide is effective in reducing RA inflammatory function by downregulating neutrophils (Zhang et al., 2017; Huang et al., 2018).

In recent years, triptolide has been mainly used for oral and parenteral administration, but it is usually detected in the organs quickly after the administration and excreted via the urinary, fecal, and biliary pathways (Gong et al., 2015; Fan et al. 2018). Due to the high toxicity of triptolide to the kidney, liver, and gastrointestinal tract, the clinical application of triptolide is significantly limited (Tan et al., 2018).

There are many advantages of transdermal drug delivery, including avoiding the gastrointestinal irritation of drugs, improving drug stability, maintaining a stable blood concentration, and achieving skin targeted therapy (such as RA). Transdermal drug delivery could deliver triptolide through the skin to the site of arthritis, thus avoiding the toxicity of triptolide. However, triptolide is a highly lipophilic lactone compound with an unstable lactone structure, which is not conducive to percutaneous absorption. Therefore, it is essential to prepare an appropriate formulation to improve the transdermal efficiency and stability of triptolide.

Targeted treatment of arthritis can be achieved by transdermal delivery; it has a broad application prospect. In this research, triptolide was prepared in a phospholipid complex and characterized. The solubilities of triptolide phospholipid complex (TPCX) in water and in ethanol were tested. Then, a TPCX cream was prepared to evaluate its percutaneous permeability, skin pharmacokinetic, and the effect on RA of rats. This study is expected to provide an experimental basis for excellent transdermal preparation of triptolide for RA (Figure 1).

CONTACT Xiu Wang  94492684@qq.com  Faculty of Pharmacy, Bengbu Medical College, Bengbu, Anhui 233030, PR China

 Supplemental data for this article can be accessed [here](#).

© 2021 The Author(s). Published by Informa UK Limited, trading as Taylor & Francis Group.

This is an Open Access article distributed under the terms of the Creative Commons Attribution-NonCommercial License (<http://creativecommons.org/licenses/by-nc/4.0/>), which permits unrestricted non-commercial use, distribution, and reproduction in any medium, provided the original work is properly cited.

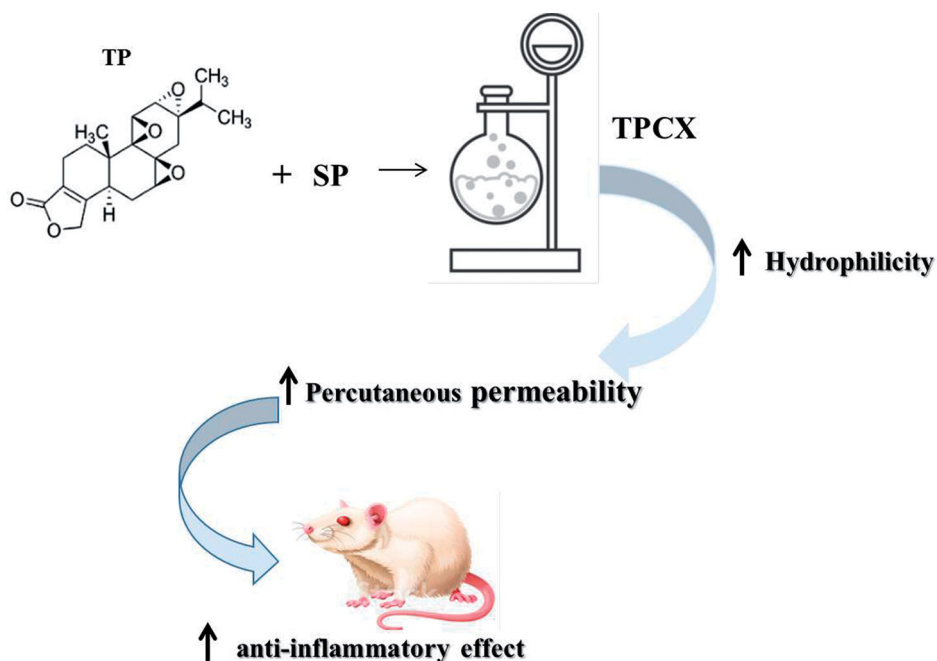


Figure 1. Scheme of triptolide phospholipid complex (TPCX) based strategy for increasing effect of triptolide (TP).

2. Materials and methods

2.1. Materials

Triptolide (L-004-181225, Chengdu Ruifinsi Biological Co., Ltd., Chengdu, China), soybean phospholipids (Tixie Shanghai Chemical Industrial Development Co., Ltd., Shanghai, China), and tetrahydrofuran (Tianjin Damao Chemical Reagent Factory, Tianjin, China) were analytically pure. Ethyl Nipagin (Shanghai Macklin Biochemical Co., Ltd., Shanghai, China), beeswax (Shanghai Macklin Biochemical Co., Ltd., Shanghai, China), glyceryl monostearate (Shanghai Macklin Biochemical Co., Ltd., Shanghai, China), white petroleum jelly (Shanghai Aladdin Biochemical Technology Co., Ltd., Shanghai, China), liquid paraffin (Shanghai Macklin Biochemical Co., Ltd., Shanghai, China), solid paraffin (Shanghai Macklin Biochemical Co., Ltd., Shanghai, China); Span 80 (Shanghai Macklin Biochemical Co., Ltd., Shanghai, China), polysorbate 80 (Hunan Er-Kang Pharmaceutical Co., Ltd., Hunan, China), BCG vaccine (Sinopharm Chemical Reagent Co. Ltd., Shanghai, China), rat TNF- α ELISA Kit (RayBiotech Life, Inc., Norcross, GA), rat IL-1 β ELISA Kit and rat IL-6 ELISA Kit (Ranjack Technology Co., Ltd., Hefei, China), methanol, and ethanol were of chromatographic pure grade.

2.2. Animals

Wistar rats, male, weighing 180–220 g, SPF grade, were purchased from Jinan Pengyue Laboratory Animal Breeding Co., Ltd. (Jinan, China) (license no.: SCXK (LU) 20190003). All the animals were adaptive fed for one week; all procedures comply with the animal ethics requirements. The animal experimental procedure was approved by the Animal Care Committee of Bengbu Medical College (license no.: 2021143) on January 19 2021.

2.3. Preparation and optimization of TPCX

2.3.1. Preparation of TPCX

First, 2.1 g of soybean phospholipid and 0.5 g of triptolide were accurately measured, and put them into the solvent of tetrahydrofuran, made the concentration of triptolide to 6.67 mg/mL, then compounded at 40 °C for 2.5 h, the solvent was removed by rotary evaporation. Thus, a compound system was obtained.

2.3.2. Encapsulation efficiency of TPCX

The prepared phospholipid complex was fully dissolved by adding chloroform and filtered using a filter paper. After drying, the filter residue was weighed to calculate the encapsulation efficiency. As triptolide is not soluble in chloroform and phospholipid complex is soluble, the amount of filter residue is the amount of unencapsulated drugs. Encapsulation efficiency was calculated using a formula as follows (Wang et al., 2015; Li et al., 2019):

$$\text{Encapsulation efficiency (\%)} = \frac{M-m}{M} \times 100\%$$

where M is the mass of triptolide in the TPCX (without precipitation) and m is the mass of undissolved triptolide.

2.3.3. Formulation and process optimization of TPCX preparation

A single-factor experiment was carried out to evaluate the effects of material ratio (mole ratio, 1:2, 1:2.5, and 1:3), formation time (2, 2.5, and 3 h), temperature (30, 40, and 50 °C), and drug concentration (6.67, 10, and 20 mg/mL) for the preparation of TPCX. Encapsulation efficiency was used as an index to optimize the prescription.

2.4. Characterization of TPCX

2.4.1. Differential scanning calorimetry (DSC) of TPCX

DSC analysis was carried out in an aluminum or Al₂O₃ crucible for reference. The temperature scanning range is 25–400 °C. The heating rate was 5 °C/min, and N₂ was used to protect the air and to purge gas (Klooster et al., 2011). Triptolide, the soybean phosphatide, the physical mixture, and phospholipid complex were analyzed by DSC (Netzsch, Selb, Germany) (Depciuch et al., 2017; Pannwitz et al., 2021).

2.4.2. Fourier-transform infrared spectroscopy (FTIR)

An appropriate amount of triptolide, soybean phospholipid, their mixture, and phospholipid complex were weighed and evenly mixed with potassium bromide. The mixture was pressed to tablets and then scanned (Hitachi, Tokyo, Japan) in the range of 4000–400 cm⁻¹ (Qian et al., 2018; Wu et al., 2018).

2.4.3. TEM and SEM images of TPCX

The microstructure of TPCX and the mixture were analyzed by transmission electron microscope (TEM) and scanning electron microscope (SEM).

2.4.4. Stability study

A certain amount of phospholipid complex is dissolved in methanol. Then, the change of the methanol solution was investigated after seven days.

2.4.5. Determination of solubility of phospholipid complex

Enough triptolide was weighed, and a physical mixture of soybean phospholipids and triptolide, and triptolide phospholipid compound were dissolved in a certain amount of distilled water or ethanol, shaken for 24 h with a table concentrator to produce a saturated solution. Then, the solution was centrifuged at 12,000 rpm for 20 min. The supernatant was collected, filtered, and diluted for HPLC analysis. A standard curve was prepared to calculate the solubility (Singh et al., 2012; Rawat et al., 2013).

2.5. Preparation of TPCX cream

The blank cream consists of glyceryl monostearate (6 g), white valentine (2 g), beeswax (2 g), liquid paraffin (10 g), solid paraffin (2 g), and SPAR 80 (0.8 g), i.e. the oil phase. Nipagin ethyl ester (0.04 g) and polysorbate 80 (0.4 g) consisted of the aqueous phase. The two phases were melted at 80 °C, and the water phase was slowly added to the oil phase. The water phase was continuously stirred at a constant temperature for 5 min and then cooled to room temperature. Thus, W/O blank cream was prepared. A prescribed amount of triptolide or TPCX was added to which preheated at 40 °C to prepare a drug-loaded W/O cream.

2.6. Percutaneous permeation study

2.6.1. HPLC analysis

The concentrations of triptolide were determined by HPLC (LC-16 Shimadzu, Kyoto, Japan). The chromatographic column consisted of a Welchrom-C₁₈ column (4.6 × 250 mm², 5 μm). Isocratic elution was performed using 40% acetonitrile and 60% ultrapure water (v/v). The flow rate was 1.0 mL/min. The detection wavelength was 219 nm. The column temperature was 35 °C. The sample size was 20 μL, and the sample was eluted with a binary high-pressure gradient elution.

2.6.2. Percutaneous permeation in vitro

The back hairs of 180–220 g Wistar rats were shaved. Then, the rats were anesthetized with ether and killed by dislocation. The skin was quickly peeled off, and the subcutaneous adipose tissue was removed. After repeated rinses with normal saline, the skins were wrapped with tin foil and placed at –20 °C for freezer storage for the preparation of isolated rat skin. Before use, they were rinsed and thawed with normal saline. The stratum corneum of rat skin was fixed upward in a Franz diffusion pool, and a certain amount of drug loaded W/O cream was applied on the skin. At the same time, 5.0 mL of PBS buffer was added to the reception room. PBS buffer was warmed to 37 °C before use, and the PBS buffer was stirred at 150 rpm and maintained at 37 °C. Then, at a given time, 0.5 mL of PBS buffer was taken to the reception room and filtered with a 0.45 μm membrane for HPLC analysis. At the same time, an equal volume of PBS buffer at 37 °C was added to the reception room.

2.6.3. Skin pharmacokinetic study

A micro dialysis (MD) system composed of a microinjection pump (BASi MD-1001, West Lafayette, IN), micro syringe with a worker controller (BASi MDN-0100, 1 mL, West Lafayette, IN), Return system (BASi, West Lafayette, IN), and Honeycomb fraction collector (BASi MD-1201, West Lafayette, IN) was used. The linear MD probe had a 30 kDa cutoff with 320 μm OD.

Skin probe implantation: The rats with back hairs were shaved and fasted without water for a night before the experiment. The depilated rats were anesthetized intraperitoneal with 25% urethane (1 mL/100 g) (Hüske et al., 2016), and 2.5 cm of length was measured in the middle part of the skin on the back of the rats using a ruler. The probe implantation point and end point were marked with a marker pen, and a skin probe was used to guide the needle to puncture the skin. The skin probe was soaked with heparin sodium and inserted with the help of a guide needle. After the probe was implanted, the implant point and end point were fixed with a medical tape to prevent the probe from moving and the drugs from entering the damaged skin. To avoid the effect of tissue fluid, a flow rate of 1 μL·min⁻¹ was used for blank perfusion (30% ethanol was diluted with normal saline) after probe implantation, and the tissue was balanced for 45 min to recover to normal level (Voelkner et al., 2019).

2.7. In vivo pharmacology study

2.7.1. Establishment of RA rat model

A rat model of RA was established by injecting heat-killed *Mycobacterium tuberculosis* suspended in mineral oil into the subplantar surface of the right hind paw of the rats. After injection, the rats were then regularly observed for signs of arthritis. The disease severity was evaluated on the basis of erythema and swelling of the paws (Wang et al., 2018, 2020; Zhou et al., 2019; Yu et al., 2020). Usually, local inflammatory reaction started in rats after immunized with heat-killed *M. tuberculosis* 1–3 days later. The injection side paw (right one) was slightly red and swollen till 12 days after immunization; the secondary side (left one) of RA rats showed redness and swelling, and gradually worsened, indicating a successful RA model. According to the above evaluation criteria, when the rats met the evaluation criteria, they were screened ($n = 6$).

2.7.2. Experimental grouping and dosing

When a rat model of RA was established, the rats were randomly divided into five groups (marked with picric acid and recorded), each group of six rats. The rats of model group were treated with blank cream. The rats of triptolide group were treated with triptolide (0.5 mg/kg) cream. The rats of TPCX cream treated group were divided into three groups: low (0.25 mg/kg), medium (0.5 mg/kg), and high (0.75 mg/kg) dose, and TPCX cream treatment was carried out separately. The cream (with the corresponding amount of triptolide) was daubed on the left posterior full ankle joint and the paw of rats. The cream was administered once every two days, and the treatment lasted for two weeks.

2.7.3. Degree of paw swelling

The paw volume of rats in each group was measured using a paw swelling meter. The rats in each group were measured for modeling (day 0), and every three days after the modeling, the degree of foot swelling was calculated using the following formula (Gowayed et al., 2015).

The degree of swelling (ΔmL) = $V_t - V_0$, where V_0 is the volume on the day before immunization (mL) and V_t is the volume on the t day after heat-killed *M. tuberculosis* immunization (Zhang et al., 2014).

2.7.4. Radiological examination

The bone mineral density, the severity of periarticular soft tissue swelling, and bone defect of rats were evaluated after 14 days of treatment. In brief, the animals were anesthetized with ether, and then the left posterior ankle joint and hind limb were examined by X-ray imaging (Multimodal Pro Light Source, Shanghai, China) (Ingawale & Patel, 2018).

2.7.5. Determination of TNF- α , IL-1 β , and IL-6

Next, 24 h after the end of the last administration, 3 mL blood was collected from the orbital venous plexus of rats in each group. After standing for 12 h, the blood was centrifuged at $3500\times g$ at 4°C for 15 min. The supernatant was

taken and stored at -20°C . The levels of TNF- α , IL-1 β , and IL-6 in the plasma were determined using ELISA kits (RayBiotech, Norcross, GA) (Sukedai et al., 2011; Wang et al., 2018; Huimin et al., 2019).

2.7.6. Histological examination and immunohistochemistry of ankle joint in rat

After the blood was collected, the rats were anesthetized with ether and then killed by dislocation. Then, the synovium of joint was collected by operation. The synovial tissue was fixed for one week, and then the paraffin-embedded sections were taken out and stained with HE (hematoxylin-eosin) staining. The results of synovial staining were observed under a microscope. Paraffin-embedded synovial tissue was sectioned, and the protein was labeled according to the immunohistochemical assay. The final immunohistochemical results were interpreted as the areas with positive brown expression observed under the microscope after DAB staining (Sun et al., 2018; Song et al., 2020).

2.8. Statistical analysis

The data were analyzed by ANOVA using SPSS 17.0 (Chicago, IL) and presented as the means \pm standard deviation (SD); $p < .05$ or $p < .01$ was regarded as a statistically significant difference.

3. Results and discussion

3.1. Single-factor experiments to optimize the formulation

3.1.1. Compound time

The ratio of soybean phospholipid to triptolide material was 2:1. The compound was prepared at 40°C for 2 h, 2.5 h, and 3 h. The encapsulation efficiencies were $(92.30 \pm 1.02)\%$, $(97.39 \pm 0.32)\%$, and $(90.30 \pm 0.98)\%$; therefore, 2.5 h was selected as the composite duration.

3.1.2. The excipients ratio

The solvent was tetrahydrofuran (10 mL). The molar ratios of triptolide:soybean phospholipid were 1:2, 1:2.5, and 1:3; the encapsulation efficiencies were $(97.39 \pm 0.34)\%$, $(96.4 \pm 0.45)\%$, and $(92.5 \pm 0.87)\%$ at 40°C for 2.5 h, respectively. The encapsulation efficiency is the highest at 1:2; therefore, the composite material ratio was selected as 1:2.

3.1.3. Compound temperature

The compound rate was $(91.80 \pm 1.23)\%$, $(96.40 \pm 0.62)\%$, and $(94.80 \pm 0.54)\%$ at 30°C , 40°C , and 50°C , respectively. The highest encapsulation efficiency was observed at 40°C .

3.1.4. The excipients concentration

According to the 1:2 ratio of triptolide to soybean phospholipid, triptolide and soybean phospholipid were weighed. Then, 5, 10, and 15 mL tetrahydrofuran was added; the drug

concentration was 20, 10, and 6.67 mg/mL, respectively. Then, the solution was heated to 40 °C for 2.5 h. The encapsulation efficiencies were (94.90 ± 1.02)%, (96.40 ± 0.46)%, and (97.90 ± 0.11)%, respectively. The results show that when the amount of solvent was 15 mL (the drug concentration was 6.67 mg/mL), the encapsulation efficiency was the highest.

Based on the results of single-factor experiments, the molar ratio of drug to soybean phospholipid was 1:2. The temperature was 40 °C; the duration was 2.5 h; and the drug concentration was 6.67 mg/mL.

3.2. Verification of TPCX

3.2.1. DSC

According to the analysis shown in Figure 2(A), an endothermic peak of triptolide appeared at 240 °C. An exothermic peak of soybean phospholipid appeared at 280 °C. The physical mixture showed both the exothermic peak of soybean phospholipids and the characteristic peak of triptolide. However, that in TPCX was not obvious. However, the characteristic peak of triptolide disappeared, and a new exothermic peak was formed near 265 °C, indicating that triptolide and its phospholipid complex had different phases.

3.2.2. Infrared

According to the results shown in Figure 2(B), the OH absorption peak of triptolide appeared at 3459.67 cm⁻¹, and the C=O absorption peak appeared at 1772.26 cm⁻¹. The C=O and P=O absorption peaks of soybean phospholipids were 1727.9 cm⁻¹ and 1452.14 cm⁻¹, respectively. The C=O absorption peak of physical mixture appeared at 1731.36 cm⁻¹, and the absorption peak of C-H appeared at 2850.2 cm⁻¹ and 2910.0 cm⁻¹. The OH absorption peak of phospholipid complex appeared at 3434.60 cm⁻¹, while the

C=O absorption peak appeared at 1739.48 cm⁻¹. After triptolide was converted into a phospholipid complex, the OH absorption peak shifted to a low wavelength direction, indicating that an intermolecular hydrogen bond might be formed between soybean phospholipid and triptolide molecules. The C=O absorption peak of phospholipid complex moved to a lower wavelength than that of triptolide, indicating that the C=O of triptolide may interact with the groups in the phospholipid.

3.2.3. Images and stability

SEM images show that TPCX is uniform and delicate, but there were many beads in PM. From the TEM images of TPCX and PM, we can know that triptolide in TPCX was dispersed as molecules or amorphous homogeneously, but in PM, triptolide was crystal state. The stability of TPCX in methanol is good. There were no visible changes after seven days.

3.3. Establishment of HPLC method for triptolide

After the implantation of skin probe, a negative skin sample was obtained by perfusion with a blank fluid. Blank perfusion solution (A) and negative skin samples (B) did not show the peak at the characteristic peak of triptolide. Compared with the control triptolide (C) and the dialyzed triptolide samples (E), they showed no interference in the determination of triptolide content.

A standard curve was drawn and determined according to the chromatographic conditions. Taking the concentration as the abscissa and the peak area as the ordinate, a standard curve equation was obtained as follows: $y = 49,568x + 11,220$, $r = 1$, indicating that the linear relationship of triptolide was good in the concentration range of 0.1–50 µg/mL.

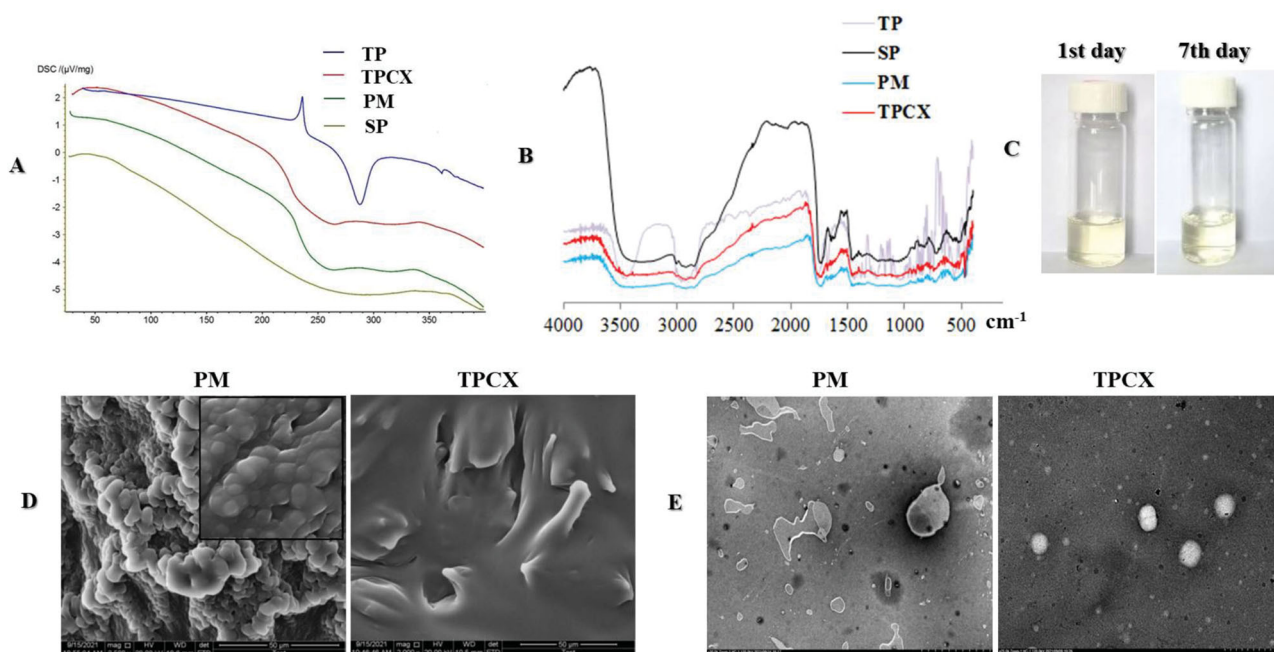


Figure 2. Characterizations of TPCX. (A) DSC spectra of triptolide (TP), soybean phospholipids (SP), Physical mixture of soybean phospholipid and triptolide (PM), and triptolide phospholipid complex (TPCX). (B) IR absorption spectra of triptolide, SP, PM, and TPCX. (C) Stability of TPCX in methanol. (D) SEM images of PM and TPCX. (E) TEM images of PM and TPCX.

Table 1. Solubility of triptolide and its phospholipid complex in water/ethanol ($\bar{x} \pm s$, $n = 3$).

Solvent	Triptolide	Physical mixture	Phospholipid complex
Distilled water (mg/mL)	0.2355 \pm 0.0017	0.2575 \pm 0.0021**	0.3179 \pm 0.0022**,#
Ethyl alcohol (mg/mL)	27.1592 \pm 2.0155	35.4227 \pm 1.8364**	40.0039 \pm 0.4775**,#

Compared to triptolide, ** $p < .01$; compared with the physical mixture, # $p < .05$, ## $p < .01$.

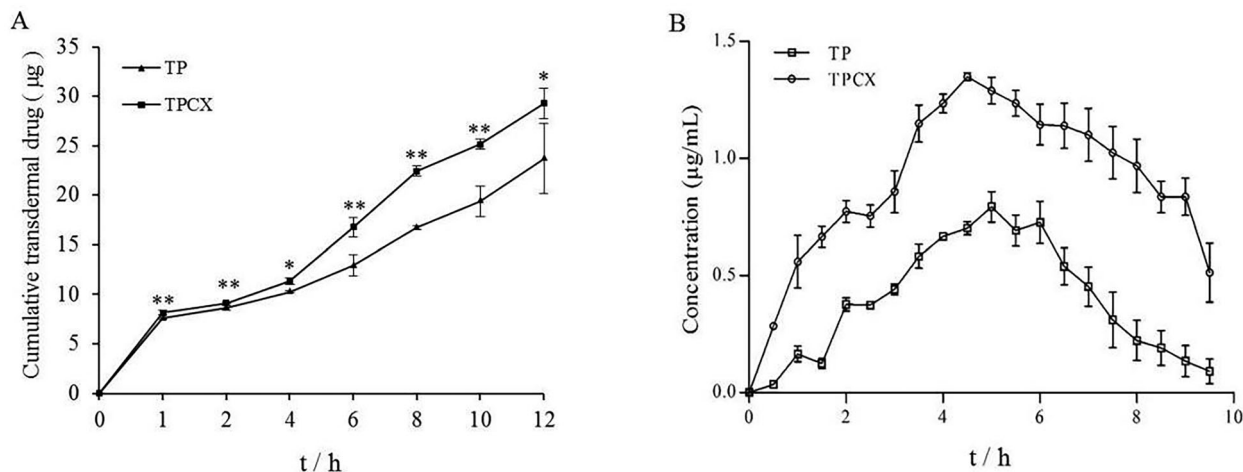


Figure 3. (A) Cumulative permeation-time curves *in vitro* ($n = 3$), * $p < 0.5$, ** $p < .01$ vs. triptolide (TP), triptolide phospholipid complex (TPCX). (B) Concentration-time curves of triptolide in skin ($n = 5$).

3.4. Solubility test

The solubility of triptolide, the physical mixture of triptolide and soybean phospholipid, the TPCX in distilled water and ethanol is shown in Table 1. The solubility of triptolide monomer in water was low; the solubility was significantly increased in the formation of phospholipid complex ($p < .01$), which was also significantly higher than that of the physical mixture group ($p < .05$). In ethanol, a semipolar solvent, the solubility of phospholipid complex was significantly higher than that of triptolide monomer and physical mixture ($p < .001$ or $p < .05$). As shown in Table 1, the solubility of physical mixture in distilled water and ethanol also increased compared with that of monomers, because soybean phospholipid is an amphiphilic substance and increases the solubility of substances. The results indicate that when triptolide compounds and soybean phospholipid form a phospholipid complex, its hydrophilicity increases, and its liposolubility decreases. On the other hand, triptolide of TPCX was dispersed in SP in molecular or/and amorphous state, which also could increase the solubility of triptolide in water or ethanol.

3.5. Transdermal absorption test

3.5.1. *In vitro* transdermal test

The results of an *in vitro* transdermal experiment are shown in Figure 3(A). The results show that the cumulative permeability amount of triptolide in phospholipid complex group was $29.32 \pm 2.16 \mu\text{g}$, but that of triptolide group was $23.72 \pm 4.60 \mu\text{g}$ within 12 h. The cumulative permeability dose per unit area was $58.64 \pm 4.32 (\mu\text{g}/\text{cm}^2)$ and $47.44 \pm 8.60 (\mu\text{g}/$

$\text{cm}^2)$, respectively. The permeability of phospholipid complex is significantly better than triptolide ($p < .05$). The transdermal permeability of triptolide in TPCX enhancement should be related to the improvement of hydrophilicity and the state of triptolide dispersed in TPCX. Permeability rate and previous seepage rate of triptolide cream and its phospholipid complexes cream were calculated, they are different (Table 2).

3.5.2. Skin pharmacokinetic study

To further prove that TPCX can improve its hydrophilicity and promote triptolide transdermal absorption, a skin pharmacokinetic study was conducted.

First, it is necessary to determine the effect of various factors on skin probe recovery *in vivo*, mainly including the flow rate and concentration of perfusion fluid. The effect of flow rate on recovery rate was calculated using the decrement method. A skin probe was placed under the skin of rat back, and $50.13 \mu\text{g}/\text{mL}$ of triptolide solution was infused at flow rates of 0.5, 1, 1.5, and $2 \mu\text{L}\cdot\text{min}^{-1}$. The results are shown in Table S1. The recovery rate of drug is inversely proportional to the flow rate, but the sample volume within half an hour should be greater than the minimum analytical volume. Therefore, the perfusion fluid with a flow rate of $1.5 \mu\text{L}\cdot\text{min}^{-1}$ was selected after comprehensive consideration. At the same time, it was found that the effect of the concentration of triptolide solution on the recovery rate was not significant; the results are shown in Table S2.

Then, microdialysis technology was used to study the real-time drug concentration of subcutaneous tissue in rats, and a drug time curve is shown in Figure 3(B). The data

were analyzed using Pharmacokinetic software Winnonlin8.1. The pharmacokinetic parameters are shown in Table 3. The AUC and peak concentration (C_{max}) of TPCX group within 9.5 h were 523.78 ± 54.24 ($\mu\text{g}\cdot(\text{mL}\cdot\text{h})^{-1}$) and 1.35 ± 0.03 ($\mu\text{g}\cdot\text{mL}^{-1}$), respectively, and those of triptolide cream group were 227.20 ± 25.79 ($\mu\text{g}\cdot(\text{mL}\cdot\text{h})^{-1}$) and 0.86 ± 0.13 ($\mu\text{g}\cdot\text{mL}^{-1}$), respectively. As for the peak time (T_{max}), the maximum concentration of TPCX group reached 4.5 h after the administration. This shows a significant rate of delivery advantage over the triptolide cream group (5.38 h). Both of them indicated that TPCX cream had better transdermal permeability and bioavailability than that of triptolide cream. In the skin pharmacokinetic study, TP and TPCX used the same base material, but the pharmacokinetic parameters are great different, this should also attribute to TPCX which could increase hydrophilicity and the solubility of triptolide in water.

Table 2. Permeability rate and previous seepage rate of triptolide and its phospholipid complexes.

Sample	Equation	$K, \mu\text{g}\cdot(\text{cm}^2\cdot\text{h})^{-1}$	kr
Triptolide	$Q = 0.6342t - 0.0017$	0.6342	1
Phospholipids complex	$Q = 0.8147 - 0.3234$	0.8147	1.2846

Table 3. Pharmacokinetic parameters of triptolide transdermal formulations ($\bar{x} \pm s, n = 5$).

PK parameters	Groups	
	TPCX cream	Triptolide cream
$AUC_{0-t}, \mu\text{g}\cdot(\text{mL}\cdot\text{h})^{-1}$	523.78 ± 54.24	227.20 ± 25.79
$AUC_{0-\infty}, \mu\text{g}\cdot(\text{mL}\cdot\text{h})^{-1}$	686.22 ± 112.27	236.27 ± 39.17
MRT_{last}, h	7.41 ± 2.36	5.11 ± 0.66
$C_{max}, \mu\text{g}\cdot\text{mL}^{-1}$	1.35 ± 0.03	0.86 ± 0.13
T_{max}, h	4.50 ± 0.02	5.38 ± 0.48
$t_{1/2}, \text{h}$	6.06 ± 0.055	4.46 ± 0.71

3.6. Effect of TPCX on the rats of RA

3.6.1. Decreased paw swelling degree in rats

The results indicate that the swelling degree of foot in RA rats did not significantly increase after immunization. As shown in Figure 4(A), during the treatment, the swelling degree of left paws of rats in the model group was significantly increased. Compared with the model group, the swelling degree of rats treated with triptolide cream or TPCX cream was significantly decreased ($p < .01$). Triptolide can reduce paw swelling and inflammation in rats. No significant statistical difference was observed between the TPCX cream medium-dose group and high dose group. Compared with the TPCX cream low-dose group and the triptolide cream group, the paw swelling in the TPCX cream medium-dose group significantly decreased ($p < .01$), because the TPCX cream medium-dose contains an equal amount of triptolide with triptolide cream group, indicating that the effect on anti-inflammation of TPCX cream was better than that of triptolide cream. The result shows that TPCX cream was more effective in alleviating inflammation than triptolide cream, probably because drug absorption was significantly improved.

3.6.2. Obvious anti-inflammatory effects by X-ray imaging

After 14 days of treatment, the bone mineral density and severity of periarticular soft tissue swelling of rats were examined by X-ray imaging. A change in bone mineral density reflects the degree of bone defect. The results indicate that after inflammation in RA rats, severe soft tissue swelling and bone local density reduction occurred in the hind limb of rats. As shown in Figure 4(C), among the model group, TPCX cream low-dose group, and triptolide cream group, all the rats had different degrees of bone defects, while both

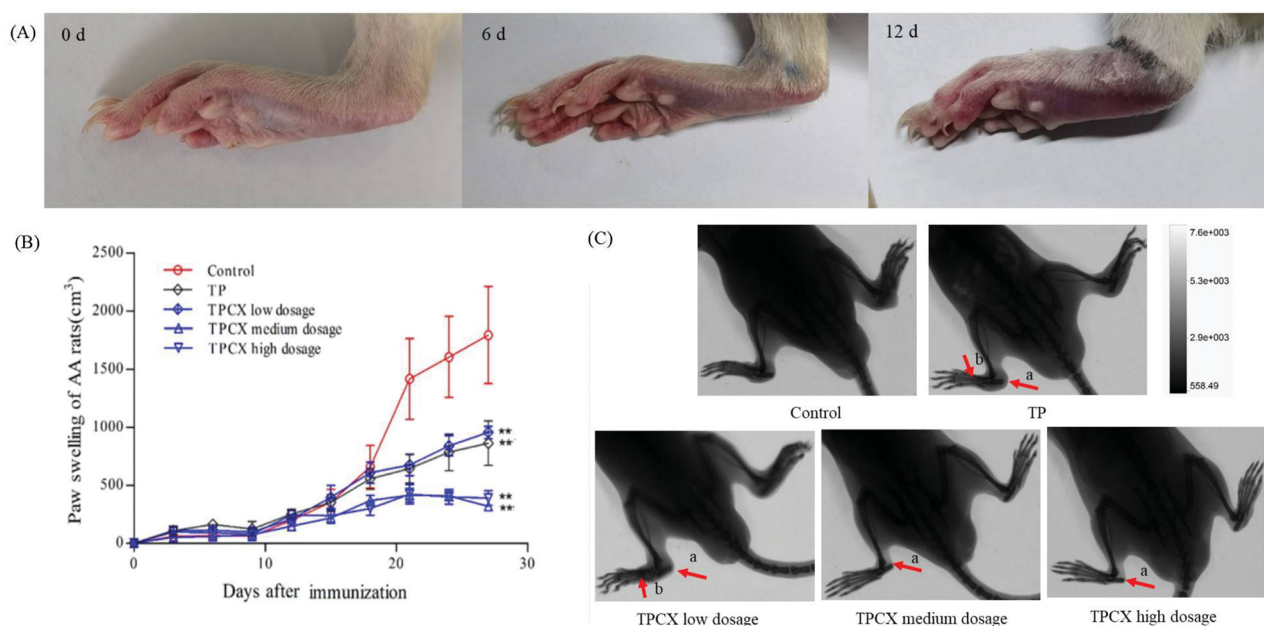


Figure 4. (A) Left paw swelling of RA rat model at day 0, day 6, and day 12 after immunization. (B) Paw swelling change of RA rat model in each group, $**p < .01$ vs. control group. (C) X-ray images of each experimental group (a, soft tissue swelling; b, bone mineral density), triptolide (TP), triptolide phospholipid complex (TPCX).

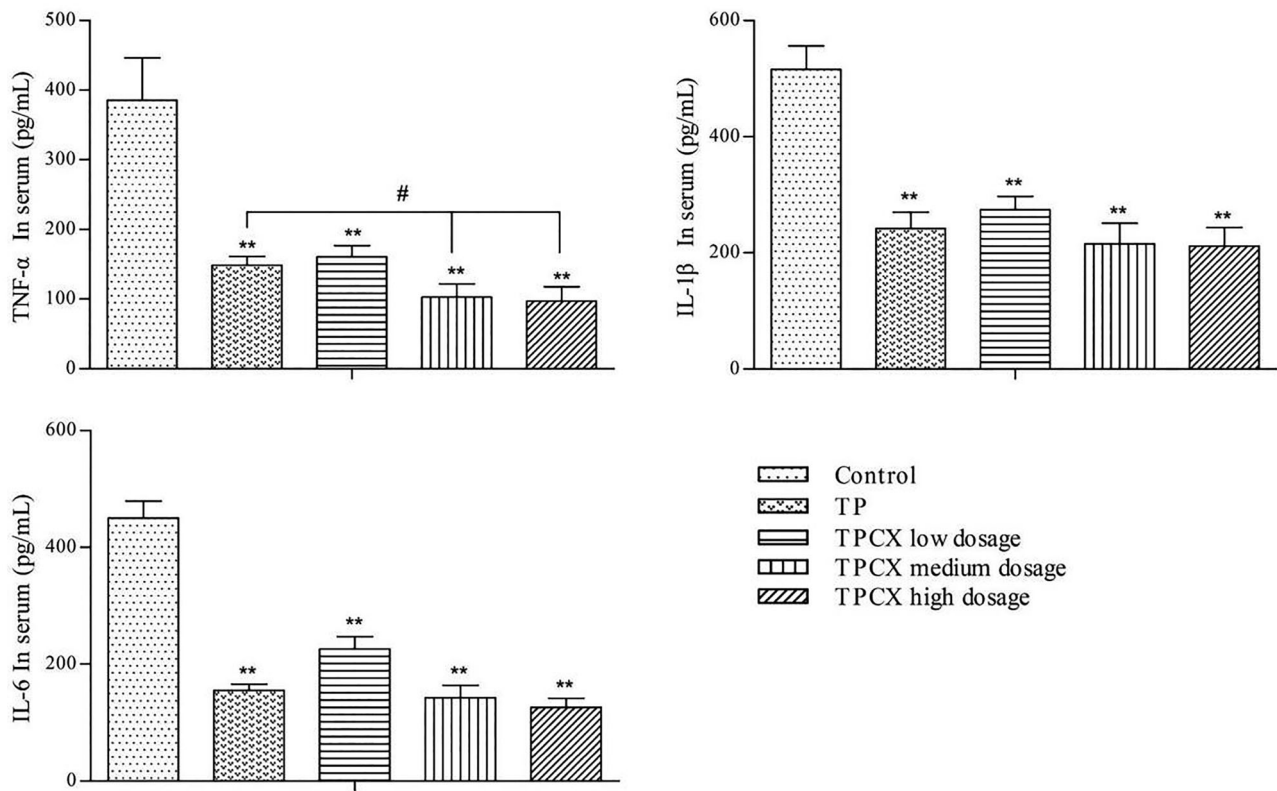


Figure 5. Levels of TNF- α , IL-1 β , and IL-6 in the serum of AA rats after treatments, ** $p < .01$ vs. control, # $p < .05$ vs. TP, triptolide (TP), triptolide phospholipid complex (TPCX).

the TPCX cream medium and high-dose group did not have bone defects, indicating that the medium and high-dose TPCX cream can effectively alleviate the progression of inflammation and avoid further bone damage of joint. Compared with the model group, the degrees of soft tissue swelling in TPCX cream low, medium, and high-dose groups decreased to a certain extent. In summary, triptolide and TPCX cream in low, medium, and high-dose groups exhibited anti-inflammation effects on RA rats, but only TPCX cream in medium and high-dose groups had the obvious protecting effect on bone.

3.6.3. Decreased level of TNF- α , IL-1 β , and IL-6 in RA rats

The proinflammatory cytokines TNF- α , IL-1 β , and IL-6 secreted by immune cells can collect a large number of neutrophils, affect the differentiation of T cells, and stimulate the abnormal activation and proliferation of fibroblast-like synoviocytes, thereby enhancing the inflammatory response and causing the injury of synovial tissue. The levels of cytokine content were detected using an ELISA kit in this experiment. Compared with the model group, the serum levels of TNF- α , IL-1 β , and IL-6 in all the treated groups significantly decreased ($p < .01$), and the level of TNF- α in rats treated with medium or high-dose TPCX cream significantly decreased compared with the triptolide cream group. The results indicate that triptolide inhibited the production of TNF- α , IL-1 β , and IL-6 in RA rats. Thus, triptolide reduced the progression of inflammation, and the paw swelling was alleviated. However, the effect on TNF- α in the serum of TPCX

cream is more significant than triptolide cream. They had an equal amount of triptolide, but the level of TNF- α was significantly reduced in TPCX cream medium dose group than triptolide cream ($p < .05$) (Figure 5).

3.6.4. Histopathological examination of synovial membrane in RA rats

The HE staining images in Figure 6 clearly show the synovial cell proliferation, pannus formation, and inflammatory cell infiltration in RA rats (Ozgen et al., 2015; Wei et al., 2016; Linghang et al., 2020). Compared with the model group, the proliferation of synovial cells and pannus in the synovial tissue was significantly reduced in the treatment groups. The results show that the synovial cell proliferation, pannus formation, and inflammatory cell infiltration decreased when the TPCX dose was increased. Meanwhile, the effect on the inhibition of synovial cell proliferation, pannus formation, and inflammatory cell infiltration of TPCX cream in medium dose was significantly stronger than triptolide cream, even when both of them contained the same amount of triptolide. The result shows that TPCX had a greater effect on the inhibition of synovial cell proliferation, pannus formation, and inflammatory cell infiltration in RA rats.

3.6.5. Expression of TNF- α and IL-6 in rats' synovial tissue

As shown in Figure 6, compared with the model group, the expression of TNF- α protein in the synovial tissue of rats in the drug treatment groups significantly decreased. These results indicate that the expression of TNF- α and IL-6 protein

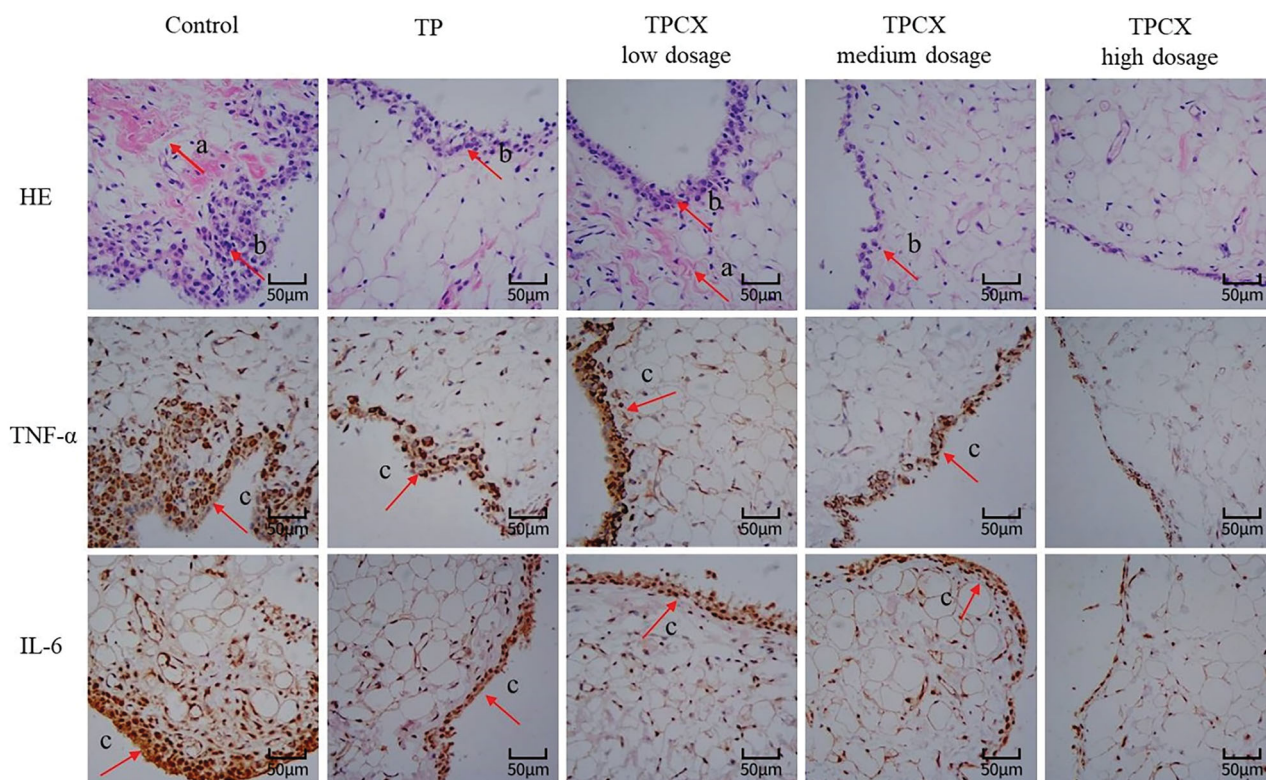


Figure 6. Histopathology and immunohistochemistry of TNF- α and IL-1 β in rat synovium (a, pannus; b, synovial cell proliferation), triptolide (TP), triptolide phospholipid complex (TPCX).

significantly increased in the synovial tissue of RA rats. Treatment with triptolide can reduce the expression of TNF- α and IL-6 protein and alleviate inflammation. TPCX showed a clear therapeutic trend in the three dose groups, and the high-dose group was the best. The expressions of TNF- α and IL-6 in triptolide and TPCX low dose group were similar. At the same drug dose, the effect of TPCX cream was significantly better than that of triptolide cream, consistent with the results of previous ELISA studies.

In this study, a phospholipid complex cream loaded with triptolide was prepared by using a complex phospholipid technology and emulsification technology. The phospholipid complex could change the hydrophilicity and solubility of triptolide. Thus, TPCX cream had a higher amount of penetration to skin and bioavailability in skin pharmacokinetic study. Finally, the triptolide-loaded phospholipid complex cream exhibited significant anti-RA effect and biological safety. The results indicate that the application of TPCX cream as a transdermal delivery carrier provides a promising approach for the treatment of RA. Further research should focus on the potential mechanism of transdermal delivery of TPCX cream.

4. Conclusions

To our knowledge, there is not any research about triptolide-phospholipid complex. The topical delivery of triptolide solid lipid nanoparticles and microemulsions was only carried out on direct effects of rats paw edema (Du et al., 2016; Mei

et al., 2003). In this study, TPCX increased the bioavailability and anti-RA effect of triptolide by increasing its hydrophilicity and transdermal permeability. In addition, the vivo pharmacology study, decreased paw swelling degree in rats, obvious anti-inflammatory effects by X-ray imaging, and decreased level of TNF- α , IL-1 β , and IL-6 in RA rats were evaluated thoroughly. The phospholipid complex can be served as an excellent form for the percutaneous absorption of triptolide. Transdermal TPCX cream provides a promising approach for the efficient treatment of RA.

Disclosure statement

The authors declared that they have no conflict of interest.

Funding

The authors appreciate the Government of China for necessary financial assistance for this work. This work was supported by the Project of Natural Science Research of Bengbu Medical College (BYKY1765), Bengbu City and Bengbu Medical College Jointed Science and Technology Key Project (BYLK201823), and the Key Project of Natural Science Research of the Education Department of Anhui Province, China (KJ2019A0348).

ORCID

Xiu Wang  <http://orcid.org/0000-0002-4988-2572>

References

- Depciuch J, Sowa-Kućma M, Nowak G, et al. (2017). The role of zinc deficiency-induced changes in the phospholipid–protein balance of blood serum in animal depression model by Raman, FTIR and UV–vis spectroscopy. *Biomed Pharmacother* 89:549–58.
- Du L, Feng X, Xiang X, Jin Y. (2016). Wound healing effect of an in situ forming hydrogel loading curcumin–phospholipid complex. *Curr Drug Deliv* 13:76–82.
- Fan D, Guo Q, Shen J, et al. (2018). The effect of triptolide in rheumatoid arthritis: from basic research towards clinical translation. *Int J Mol Sci* 19:376.
- Feldmann M. (2002). Development of anti-TNF therapy for rheumatoid arthritis. *Nat Rev Immunol* 2:364–71.
- Gong X, Chen Y, Wu Y. (2015). Absorption and metabolism characteristics of triptolide as determined by a sensitive and reliable LC–MS/MS method. *Molecules* 20:8928–40.
- Gowayed MA, Refaat R, Ahmed WM, El-Abhar HS. (2015). Effect of galantamine on adjuvant-induced arthritis in rats. *Eur J Pharmacol* 764: 547–53.
- Huang G, Yuan K, Zhu Q, et al. (2018). Triptolide inhibits the inflammatory activities of neutrophils to ameliorate chronic arthritis. *Mol Immunol* 101:210–20.
- Huimin D, Hui C, Guowei S, et al. (2019). Protective effect of betulinic acid on Freund's complete adjuvant-induced arthritis in rats. *J Biochem Mol Toxicol* 33:e22373.
- Hüske C, Sander SE, Hamann M, et al. (2016). Towards optimized anesthesia protocols for stereotactic surgery in rats: analgesic, stress and general health effects of injectable anesthetics. A comparison of a recommended complete reversal anesthesia with traditional chloral hydrate monoanesthesia. *Brain Res* 1642:364–75.
- Ingawale DK, Patel SS. (2018). Hecogenin exhibits anti-arthritis activity in rats through suppression of pro-inflammatory cytokines in Complete Freund's adjuvant-induced arthritis. *Immunopharmacol Immunotoxicol* 40:59–71.
- Klooster KL, Burrueel VR, Meyers SA. (2011). Loss of fertilization potential of desiccated rhesus macaque spermatozoa following prolonged storage. *Cryobiology* 62:161–6.
- Li B, Han L, Cao B, et al. (2019). Use of magnoflorine-phospholipid complex to permeate blood-brain barrier and treat depression in the CUMS animal model. *Drug Deliv* 26:566–74.
- Li X, Mao Y, Li K, et al. (2016). Pharmacokinetics and tissue distribution study in mice of triptolide-loaded lipid emulsion and accumulation effect on pancreas. *Drug Deliv* 23:1344–54.
- Linghang Q, Yiyi X, Guosheng C, et al. (2020). Effects of atractylodes oil on inflammatory response and serum metabolites in adjuvant arthritis rats. *Biomed Pharmacother* 127:110130.
- Liu Q. (2011). Triptolide and its expanding multiple pharmacological functions. *Int Immunopharmacol* 11:377–83.
- Malahias M, Gardner H, Hindocha S, et al. (2012). The future of rheumatoid arthritis and hand surgery – combining evolutionary pharmacology and surgical technique. *Open Orthop J* 6:88–94.
- Mei Z, Chen H, Weng T, et al. (2003). Solid lipid nanoparticle and microemulsion for topical delivery of triptolide. *Eur J Pharm Biopharm* 56: 189–96.
- Ozgen M, Koca SS, Karatas A, et al. (2015). Lapatinib ameliorates experimental arthritis in rats. *Inflammation* 38:252–9.
- Pannwitz A, Saaring H, Beztsinna N, et al. (2021). Mimicking photosystem I with a transmembrane light harvester and energy transfer-induced photoreduction in phospholipid bilayers. *Chemistry* 27:3013–8.
- Qian Y, Chen G, Wang J, Ren L. (2018). Preparation and evaluation of probucol-phospholipid complex with enhanced bioavailability and no food effect. *AAPS PharmSciTech* 19:3599–608.
- Rawat DS, Thakur BK, Semalty M, et al. (2013). Baicalein–phospholipid complex: a novel drug delivery technology for phytotherapeutics. *Curr Drug Discov Technol* 10:224–32.
- Singh D, Rawat MS, Semalty A, Semalty M. (2012). Rutin–phospholipid complex: an innovative technique in novel drug delivery system – NDDS. *Curr Drug Deliv* 9:305–14.
- Song X, Zhang B, Taorong W, et al. (2020). Effects of cyclopamine on the viability of articular chondrocytes in rats with adjuvant arthritis in vitro. *Ann Clin Lab Sci* 50:85–91.
- Sukedai M, Ariyoshi W, Okinaga T, et al. (2011). Inhibition of adjuvant arthritis in rats by electroporation with interleukin-1 receptor antagonist. *J Interferon Cytokine Res* 31:839–46.
- Sun Y, Zhao D, Liu Z, et al. (2018). Inhibitory effect of salvianolic acid on inflammatory mediators of rats with collagen-induced rheumatoid arthritis. *Exp Ther Med* 16:4037–41.
- Tan QY, Hu Q, Zhu SN, et al. (2018). Licorice root extract and magnesium isoglycyrrhizinate protect against triptolide-induced hepatotoxicity via up-regulation of the Nrf2 pathway. *Drug Deliv* 25:1213–23.
- Voelkner N, Voelkner A, Derendorf H. (2019). Determination of dermal pharmacokinetics by microdialysis sampling in rats. *Curr Protoc Pharmacol* 85:e58.
- Wang H, Cui Y, Fu Q, et al. (2015). A phospholipid complex to improve the oral bioavailability of flavonoids. *Drug Dev Ind Pharm* 41: 1693–703.
- Wang Y, Wei Y, Cheng X, et al. (2018). *J South Med Univ* 38:962–8.
- Wang Y, Xian H, Qi J, et al. (2020). Inhibition of glycolysis ameliorate arthritis in adjuvant arthritis rats by inhibiting synoviocyte activation through AMPK/NF- κ B pathway. *Inflamm Res* 69:569–78.
- Wang ZZ, Liu F, Gong YF, et al. (2018). Antiarthritic effects of sorafenib in rats with adjuvant-induced arthritis. *Anat Rec* 301:1519–26.
- Wei F, Xu S, Jia X, et al. (2016). BAFF and its receptors involved in the inflammation progress in adjuvant induced arthritis rats. *Int Immunopharmacol* 31:1–8.
- Wu JY, Li YJ, Han M, et al. (2018). A microemulsion of puerarin–phospholipid complex for improving bioavailability: preparation, in vitro and in vivo evaluations. *Drug Dev Ind Pharm* 44:1336–41.
- Yang M, Feng X, Ding J, et al. (2017). Nanotherapeutics relieve rheumatoid arthritis. *J Control Release* 252:108–24.
- Yu Y, Cai W, Zhou J, et al. (2020). Anti-arthritis effect of berberine associated with regulating energy metabolism of macrophages through AMPK/HIF-1 α pathway. *Int Immunopharmacol* 87:106830.
- Zhang S, Huang G, Yuan K, et al. (2017). Tanshinone IIA ameliorates chronic arthritis in mice by modulating neutrophil activities. *Clin Exp Immunol* 190:29–39.
- Zhang W, Zhang J, Zhang M, Nie L. (2014). Protective effect of *Asarum* extract in rats with adjuvant arthritis. *Exp Ther Med* 8:1638–42.
- Zhou J, Yu Y, Yang X, et al. (2019). Berberine attenuates arthritis in adjuvant-induced arthritic rats associated with regulating polarization of macrophages through AMPK/NF- κ B pathway. *Eur J Pharmacol* 852: 179–88.